

Stick-slip dynamics in the relaxation of stresses in a continuous elastic medium

Miguel A. Rubio¹ and Javier Galeano^{1,2}

¹*Departamento de Física Fundamental, Universidad Nacional de Educación a Distancia, Apartado 60141, Madrid 28080, Spain*

²*Departamento de Ciencia Aplicada a la Ingeniería Técnica Agrícola, Universidad Politécnica de Madrid, Madrid 28040, Spain*

(Received 23 March 1994)

We report on experimental results on the dynamical behavior of the stress relaxation in a model system for earthquakelike dynamics. In the experiments, a continuous elastic medium, namely, a transparent gel, is sheared at a very slow rate in between two coaxial circular cylinders. The stress relaxations are investigated locally by means of photoelastic techniques. We find four different stick-slip dynamical regimes. Three of them are reminiscent of the unstable solutions of the Burridge-Knopoff model: the sliding, the global relaxation, and the solitonlike propagating solutions. The fourth regime shows complex spatiotemporal behavior involving events of all sizes. For this last type of behavior the statistics of event duration, event separation, and amplitude show exponential behavior.

PACS number(s): 05.45.+b, 91.30.Dk, 05.40.+j

I. INTRODUCTION

Avalanching and stick-slip behavior are two interesting cases of complex spatiotemporal dynamics that may appear in extended systems. The fact that they appear to share many of their dynamical features is particularly remarkable and, in this spirit, two physical systems showing these types of behavior have received much attention recently. Sandpiles have been investigated both by means of computer automata [1] and experimentally [2,3]. The idea that has motivated these studies is the search for self-organized criticality, which should show up as nontrivial power-law statistics or $1/f$ power spectra. Numerical simulations of sandpile automata yield the expected scale invariant statistics and power spectra [4]. However, experiments on real sandpiles apparently suggest that these nontrivial statistics appear only for small size sandpiles [3,5].

On the other hand, the investigation of the mechanisms of earthquake production and their possible relationship with stick-slip instabilities has excited a great amount of work [6]. Fully deterministic spring-block models with velocity weakening friction [7–9] appear to be a particularly interesting case. The physical ingredients of these models are a couple of plates in uniform relative motion and a chain of blocks that are elastically coupled among themselves and to one of the plates and sliding on top of the other plate with a velocity-weakening friction force.

Numerical studies of these models have shown that several types of complex spatiotemporal dynamics may appear, depending on the different length and velocity scales of the system. For instance, a scale invariant regime in which events have no preferred time or length scale has been thoroughly studied [8,9]. The series of events in these regimes show power-law statistics in good agreement with the Gutenberg-Richter law [10] for the existing data on real earthquakes. On the other

hand, nearly periodic global relaxations dominate the dynamics [11] when the velocity scale appearing in the velocity weakening friction is greater than the pulling speed. Propagating solutions exist also in systems with periodic boundary conditions [9] and their existence depends on both the size of the system and the pulling rate [12]. An extension of the model to two dimensions with coupling through a viscous fluid shows both the Gutenberg-Richter law and the power-law decay of aftershocks (Omori's law) [13]. Some attempts have been made also to develop continuous models which might show repetitive stick-slip dynamics [14,15].

To our knowledge the only experimental study in which local spatiotemporal information is available has been performed in a system in which a glass rod is pulled on top of a latex membrane [16]. In this system the slipping events appear as detachment waves and there is a wide distribution of event sizes. However, robust scaling behavior was not found.

Here we report on experiments performed in a continuous elastic system sheared between two coaxial circular cylinders. The inner cylinder is rotated at very low angular speed and the cell is filled with a transparent gel providing for a highly deformable mainly elastic medium [17]. In that way the system closely resembles the physics of a spring-block model with periodic boundary conditions, although the actual form of the friction law is not known in detail. Furthermore, the use of photoelastic imaging techniques allows us to have local information about the spatiotemporal dynamics of the system.

The paper is organized as follows. In Sec. II we describe the experimental setup, the physical properties of the gels used, and the stress building process in a typical experiment. In Sec. III we describe the four different dynamical regimes found in the experiment, including a brief comparison with similar regimes found in simulations of the Burridge-Knopoff model. Finally, in Sec.

IV we state some brief conclusions on the experimental results and comment on further studies and some open questions.

II. EXPERIMENTAL SETUP

A sketch of the experimental setup is shown in Fig. 1. We carried out our experiments in an annular cell made of two parallel plates an external cylindrical wall, and an inner rotor. The two parallel plates, and the external cylindrical wall were made in Plexiglas. We used three different inner cylinders made on Teflon, Plexiglas and stainless steel to allow for different friction forces at the slipping interface. The height of the cell was 1.5 cm and the inner and outer radii were 2 cm and 5 cm, respectively. The inner cylinder was slowly rotated by a stepper motor with a resolution of 25 000 steps/rev and with angular velocities down to $2.5 \times 10^{-4} \text{ sec}^{-1}$ (corresponding to 1 step/sec). Therefore the minimal linear velocity at the surface of the rotor was $5.0 \times 10^{-4} \text{ cm sec}^{-1}$.

We used different gels [18,19] made of aqueous solutions of gelatin (Fluka 48724) in concentrations up to 20% by weight or mixtures of the same gelatin and agarose (Sigma A-6877) in concentrations up to 10% and 1% by weight, respectively. Just to give an order of magnitude, the modulus of elasticity of a 15% aqueous gelatin gel at 20 °C is about $8 \times 10^4 \text{ Pa}$ [19]. The gels were prepared by heating the solutions up to 70 °C in a magnetic stirrer, filling up the cell with the solution and cooling down the cell to 20 °C in a temperature controlled bath. Experiments started after 12 h of curing time. Gels with no significant initial stresses were produced with this procedure.

Composition strongly affects the relevant physical properties of the gels even in the small range of variation stated above. For instance, gels made of gelatin only showed good friction properties, but barely enough rigidity to withstand the stresses developed in the corners formed by the parallel plates and the rotor. Adding agarose increased significantly the gel rigidity, but it apparently developed a kind of lubrication layer, therefore diminishing friction at the slipping surface.

The optical setup was made of an annular fluorescent lamp, a diffusor (*D*), and two linear polarizers (*P*, *A*) placed in a crossed configuration [20]. In that way the output light field contains two different kinds of information. First, the intensity carries information about the

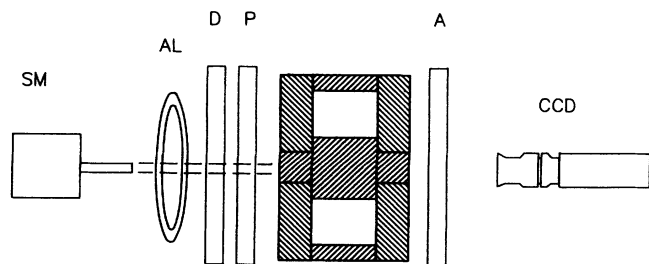


FIG. 1. Experimental setup: SM, stepper motor; AL, annular lamp; *D*, diffusor; *P*, polarizer; *A*, analyzer; CCD, video camera.

orientation of the local principal stress directions relative to the orientation of the polarizers. The lines corresponding to points with equal orientations with respect to the polarizers are called isoclinics. In the present geometry they appear mainly as a cross made of four dark bands that are shifted by $\frac{\pi}{4}$ with respect to the polarizers, which are oriented along the horizontal and vertical axes of the system. Second, the color depends on the difference between the local values of the principal stresses. Equal differences give rise to lines of equal color which are called isochromics.

The output light field was captured with a color charge coupled device (CCD) camera (SONY DXC-151) with the shutter triggered synchronously with the power supply of the fluorescent lamp. The video images were digitized directly from the camera output, by means of a color digitizing system with eight bit resolution for each color component, into frames of 720×578 pixels. The final spatial resolution was about 0.1 mm. The time interval between consecutive images was 0.6 sec, which proved to be short enough to capture the time scales of the stress relaxations. Finally, we transformed the digitized data from red-green-blue (RGB) format to hue-saturation-intensity (HSI) coding because it proved to be more convenient for the analysis of the data.

Due to the friction of the gel against the plates the stress field is three dimensional. Furthermore, the optical information is integrated along the axis of the system and therefore the actual local values of the stresses cannot be recovered from the planar light field. However, changes in intensity and/or color reveal changes in the local stress field and therefore these changes may be used to study the spatiotemporal behavior of the stress relaxations in the system.

The evolution in a typical experiment is as follows. Initially the part of the gel that is in contact with the rotor is entrained by the rotor motion and stresses are built into the gel. Again, due to the influence of the plates, the stresses affect only a small layer in the vicinity of the rotor surface, whose depth is always smaller than one-third of the radial span of the cell. The stresses in the gel increase until they are greater than the static friction at some position in the gel-rotor interface. Then that part of the gel moves with respect to the rotor and some amount of stress is relaxed. We have no evidence of the presence of detachment waves in these stress relaxation events within the resolution of our system. Instead, these processes apparently occur through actual slip motion of the gel at its boundary. Another important observation is that the stress relaxed in these events is never large enough to take the system back again to the initial unstressed state. That might be interpreted in the sense that the friction force takes a nonzero value at high slipping speeds.

These stress relaxation events may extend to the whole interface or remain localized. The process of stress building and successive relaxations is generally repeated and gives rise to stick-slip dynamics. To analyze the spatiotemporal behavior of the system we have taken advantage of the stress localization near the gel boundary. In fact, we have taken the information corresponding to

points located in a circle concentric with the section of the rotor and with slightly higher radius (typically 1 mm higher). In such a way we are left with the angular coordinate only, but the spatiotemporal behavior is well represented because everything happens close to the rotor boundary.

III. RESULTS

By changing the gel's rigidity and friction properties and the rotor angular speed we have found four main types of spatiotemporal behavior. When using the Teflon rotor and a mixture gel, an axisymmetric stress field is built initially until the friction threshold is attained. Then the gel starts to slip at the boundary at the pulling speed relative to the rotor and maintaining the stress field existing before slippage started. This type of evolution is similar to the analytical solution of the Burridge-Knopoff (BK) model in which the blocks are moving uniformly at the pulling speed relative to the rough surface [9]. However, this solution of the BK model is linearly unstable against perturbations of any wavelength. The fact that it appears when using the Teflon rotor suggest that friction against the Teflon rotor might depend very little on the rotor speed.

When using steel or Plexiglas rotors three other dynamical regimes may appear. Two of them are illustrated by the plots of the spatiotemporal evolution in Figs. 2(a) and 2(b). These plots show the evolution of the contrast enhanced light intensity at each point in a circle with ra-

dius 1 mm larger than that of the rotor. In this way the history of the intensity at each point is represented along horizontal lines and sudden changes in intensity represent strong stress relaxations. The different base intensities along each horizontal line are due to the isoclinics.

In Fig. 2(a) we show the evolution for a gel made of 8% gelatin and 0.4% agarose, sheared at $5.0 \times 10^{-4} \text{ sec}^{-1}$ with a steel rotor. Under these conditions global relaxations occur, i.e., when a relaxation event starts it quickly propagates through the whole cell. After some time another similar event occurs. This series of events is nonperiodic, but has a well defined time scale of about 55 sec. This regime is reminiscent of the unstable periodic spatially uniform global relaxation solution of the BK model, in which all blocks move simultaneously the same distance and at equal time intervals [9]. Similar global event regimes have been found also in numerical simulations [11] when friction is independent of velocity.

Figure 2(b) corresponds to the same rotation speed as Fig. 2(a), but with a slightly more rigid gel. In this case a regime of propagating relaxation appears. This can be noticed as the reentrance of the relaxation at $\phi = 0$ each time it goes out at $\phi = 2\pi$. The time scale corresponding to the loading period in the BK model has been lowered with respect to the previous case and it becomes comparable to the time that it takes for the relaxation to propagate through the whole cell. This regime is reminiscent of the propagating soliton solution of the BK model described analytically in [9] and studied numerically [12]. According to [9] this analytic solution should be unstable too, although Schmittbuhl *et al.* have shown that it appears to be stable in numerical simulations. Once again the experimental regime is nonperiodic, although the time scale is well defined and allows one to calculate an average propagation speed of about 0.35 cm/sec. This propagation speed is separated by more than two orders of magnitude from the linear speed of the rotor boundary, which is 0.001 cm/sec.

An interesting regime that shows events in many time and amplitude scales appears for softer gels. Such an evolution may be appreciated in the time series shown in Fig. 3, which corresponds to the local intensity in the

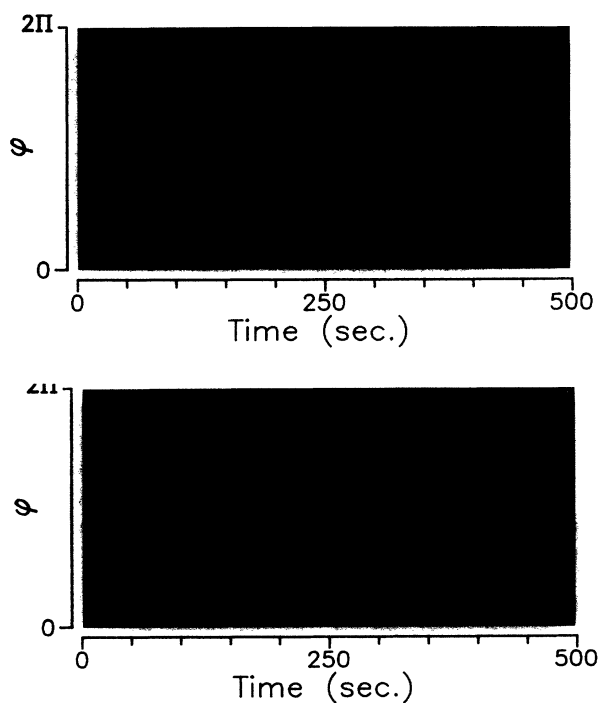


FIG. 2. Spatiotemporal evolution of the intensity. The near vertical bands shown by intensity changes correspond to the relaxations. (a) Nonperiodic global relaxation regime. (b) Propagating relaxation.

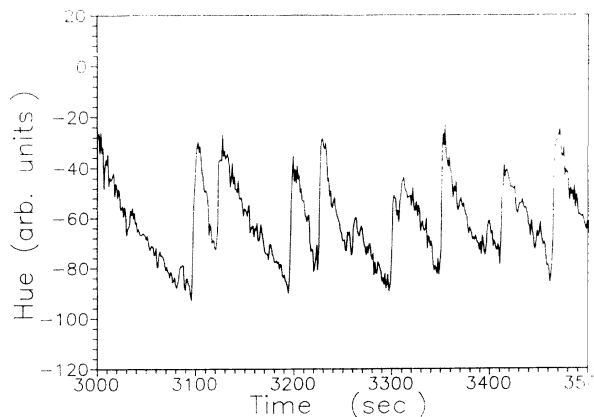


FIG. 3. Detail of the time evolution of the intensity for a 10% gelatin gel with a Plexiglas rotor moving at a rate of $2.5 \times 10^{-4} \text{ sec}^{-1}$.

case of a 10% gelatin gel sheared at $2.5 \times 10^{-4} \text{ sec}^{-1}$ with a Plexiglas rotor. Large events appear separated by a still well defined time scale of about 60 sec. However, small amplitude events also appear in between large events.

We have performed a statistical analysis of the data. Unfortunately, the intensity is very low in the four dark isoclinics previously mentioned. Therefore, the signal to noise ratio in those regions is very poor and it is not possible to follow the relaxations across them. Consequently, we have been forced to make local statistics based on time series such as the one shown in Fig. 3. The statistics have been computed in time series ranging from 10 000 to 20 000 sec. The typical number of events in such runs is about 1000. All of the statistics have been performed using different threshold values to locate the starting and ending points of an event. The results reported here correspond to an amplitude threshold of approximately twice the noise in the amplitude signal and they are insensitive to small upward changes in the threshold parameter.

We have chosen to represent the integrated probability distributions, i.e., the normalized number of events whose size A' (duration or separation T') is greater than size A (duration or separation T). For limited data sets this is a more convenient function to distinguish between exponential or power-law statistics. The amplitude integrated probability distribution for the whole time series corresponding to a 15% gelatin gel sheared at $5.0 \times 10^{-4} \text{ sec}^{-1}$ with a Plexiglas rotor is shown in Fig. 4. Apart from small deviations at very small and very high amplitudes an exponential character appears, pointing at a non-scale-invariant regime. To our knowledge all of the detailed studies reported on the BK model refer to the scale invariant regime, although exponential regimes may be found too [21]. However, this result should not be pushed too far because in this experiment intensity is not a linear function of local stress or strain.

On the other hand, temporal statistics are much more conclusive. Figure 5 shows the integrated probability dis-

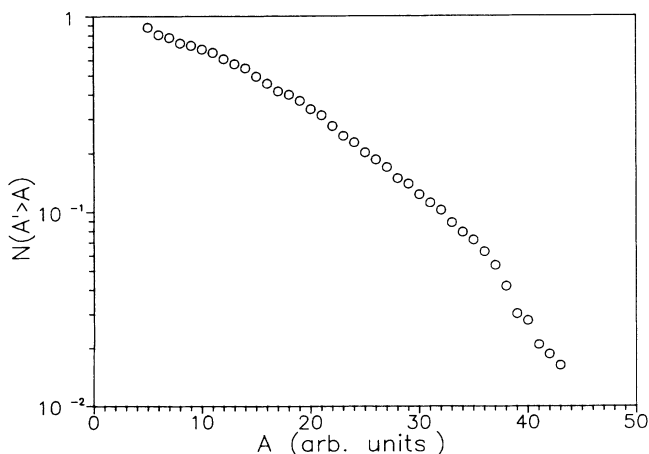


FIG. 4. Amplitude integrated probability distribution for the whole time series corresponding to a 15% gelatin gel with Plexiglas rotor, sheared at $5.0 \times 10^{-4} \text{ sec}^{-1}$.

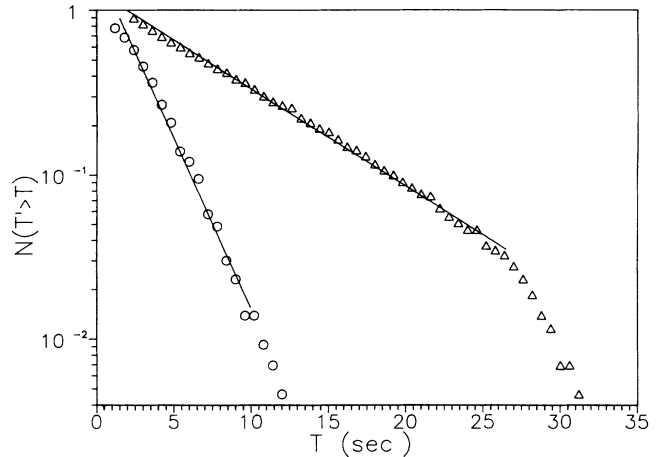


FIG. 5. Integrated probability distributions for event duration (circles) and separation between successive events (triangles), at the same conditions as in Fig. 4. Straight lines correspond to least-squares fits.

tributions for the duration of the events (circles) and the time elapsed between consecutive events (triangles) for the same time series as Fig. 4. The straight lines correspond to least-squares fits for times below 12 and 26 sec, respectively. Both of them show exponential decay with different time constants: 7.4 ± 0.2 for the durations and 2.1 ± 0.2 for the time intervals, where the error bar corresponds to the standard deviation for several runs in the same conditions. Furthermore, the interval statistics shows a crossover at about 27 sec, above which the slope of the integrated probability distribution increases, which means that region has a higher probability density. We are not aware of similar data to compare with in the literature on the BK model.

The existence of a typical time scale for the duration of events is not very surprising because the viscoelastic properties of the gel must set up a typical decay time for stress perturbations. The situation is not so clear for the interval statistics. In the BK model the only time scale that can be established concerning the separation of events is the time that it takes for a pulling spring to build an elastic force equal to the static friction. This time scale should show up as an upper cutoff value for the separation between events and eventually with an increased probability for time intervals slightly smaller than this cutoff rather than as a time constant in the probability distribution.

IV. CONCLUSION

Summarizing, we have carried out experiments in a continuous elastic medium which show stick-slip dynamics in different regimes. Three of these regimes, the stable slippage, the nonperiodic global relaxations, and the propagating relaxation, are reminiscent of the unstable

analytical solutions of the BK model. The fourth regime, which involves events in many amplitude and time scales, shows exponential statistical features in amplitude, duration, and separation between events. This is at variance with the published results on the BK model where published results refer to scale-invariant statistics, at least as far as event magnitude is concerned.

Many aspects of the problem deserve further investigation, such as the influence of the viscoelastic properties of the gels on the dynamics or the actual form of the friction law at the boundary. Studies of issues such as to what extent the present results might be affected by

finite cell size or an analysis of the time series in terms of aftershocks are presently being done.

ACKNOWLEDGMENTS

We thank D. Vallette, J. P. Gollub, P. Español, and M. de Sousa Vieira for helpful discussions. We also thank J. M. Pastor for very efficient technical assistance. This work has been supported by DGICYT, Project No. PB89-0196, and Comunidad de Madrid, Project No. CO85-90.

-
- [1] P. Bak, C. Tang, and K. Wiesenfeld, *Phys. Rev. Lett.* **59**, 381 (1987).
 - [2] H. M. Jaeger, C.-H. Liu, and S. R. Nagel, *Phys. Rev. Lett.* **62**, 40 (1989).
 - [3] G. A. Held, D. H. Solina II, D. T. Keane, W. J. Haag, P. M. Horn, and G. Grinstein, *Phys. Rev. Lett.* **65**, 1120 (1990).
 - [4] C. Tang and P. Bak, *Phys. Rev. Lett.* **60**, 2347 (1988).
 - [5] S. R. Nagel, *Rev. Mod. Phys.*, **64**, 321 (1992).
 - [6] C. H. Scholz, *The Mechanics of Earthquakes and Faulting* (Cambridge University Press, Cambridge, 1990).
 - [7] R. Burridge and L. Knopoff, *Bull. Seismol. Soc. Am.* **57**, 341 (1967).
 - [8] J. M. Carlson and J. S. Langer, *Phys. Rev. Lett.* **62**, 2632 (1989).
 - [9] J. M. Carlson and J. S. Langer, *Phys. Rev. A* **40**, 6470 (1989).
 - [10] B. Gutenberg and C. F. Richter, *Ann. Geofis.* **9**, 1 (1956).
 - [11] M. de Sousa Vieira, G. L. Vasconcelos, and S. R. Nagel, *Phys. Rev. E* **47**, 2221 (1993).
 - [12] J. Schmittbuhl, J. P. Vilotte, and S. Roux, *Europhys. Lett.* **21**, 377 (1993); P. Español, *Phys. Rev. E* **50**, 227 (1994).
 - [13] H. Nakanishi, *Phys. Rev. A* **46**, 4689 (1992).
 - [14] R. Burridge, and G. S. Halliday, *Geophys. J. R. Astron. Soc.* **25**, 261 (1971).
 - [15] R. Burridge, *J. Geophys. Res.* **82**, 1663 (1977).
 - [16] D. P. Vallette and J. P. Gollub, *Phys. Rev. E* **47**, 820 (1993).
 - [17] J. D. Ferry, *Adv. Protein Chem.* **4**, 1 (1948).
 - [18] J. D. Ferry, *Viscoelastic Properties of Polymers* (John Wiley and Sons, New York, 1980).
 - [19] J. L. Laurent, P. A. Jamney, and J. D. Ferry, *J. Rheol.* **24**, 87 (1980).
 - [20] A. Kuske, *Photoelastic Stress Analysis* (John Wiley and Sons, New York, 1974).
 - [21] M. de Sousa Vieira (private communication).

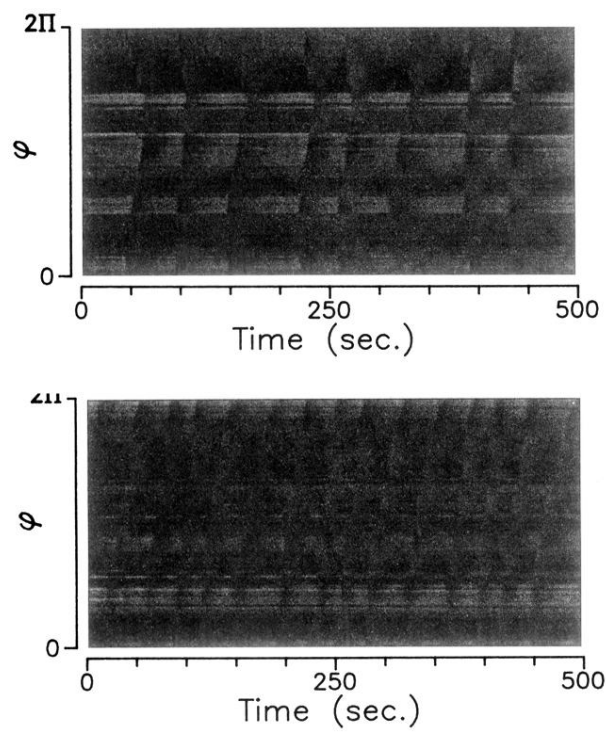


FIG. 2. Spatiotemporal evolution of the intensity. The near vertical bands shown by intensity changes correspond to the relaxations. (a) Nonperiodic global relaxation regime. (b) Propagating relaxation.